Supplementary Information

Abnormal Anti-thermal Quenching of Mn^{2+} and Reverse Thermal Response of Mn^{2+}/Mn^{4+} Luminescence in Garnet Phosphor for Wide-range Temperature Sensing

Annu Balhara,[1,2] Santosh K. Gupta,[1,2*] G. D. Patra,[3] Boddu S. Naidu,[4] Kathi Sudarshan[1,2]

[1]*Radiochemistry Division, Bhabha Atomic Research Centre, Trombay, Mumbai-400085, India*
[2]*Homi Bhabha National Institute, Anushaktinagar, Mumbai – 400094, India*
[3]*Technical Physics Division, Bhabha Atomic Research Centre, Trombay, Mumbai-400085, India*
[4]*Institute of Nano Science and Technology, Mohali-140306, India*

**To whom correspondence should be addressed. Electronic mail: *santoshg@barc.gov.in/ santufrnd@gmail.com (SKG)*

S1. Experimental Section

S1.1. Synthesis

A series of YAGG: $x\text{Mn}^{2+/4+}$ (x = 0.002, 0.005, 0.02, 0.04 and 0.06 mol) phosphors was synthesized by a two-step high-temperature solid-state method. The raw materials, Y_2O_3 (99.99%), Al_2O_3 (AR), Ga_2O_3 (AR), and $MnCO_3$ (AR) were weighed in stoichiometric amounts and mixed homogeneously by grinding for 25 min using an agate mortar and pestle. Then, the fine mixture was preheated at 1200 ^oC for 15 h in a tubular furnace in air atmosphere. Following this, the powder samples were annealed at 1400 ^oC for 15 h in air after an intermittent grinding for 15 min. After cooling, all the samples were ground well into fine powder for further characterization and studies.

S1.2. Instrumentation

The powder XRD patterns were acquired on a Proto-AXRD bench top system in the 2θ range of 15-80° and a scan rate of 1°/min. Fourier Transform Infrared Spectroscopy (FTIR) was performed with a diamond ATR mode on a Bruker Alpha FTIR spectrometer in the scanning range from 500 to 4000 cm^{-1}. The energy dispersive spectroscopy (EDS) was performed on a SEM (Model: JEOL ICM6000Plus-7E, Japan) system. Transmission electron microscopy (TEM) measurements were done on a JEOL, JEM-2100 TEM microscope with an operating voltage of 200 kV. The PL and PLE spectra were recorded with a continuous Xenon lamp

(450 W) source on a FLS-1000 fluorescence spectrometer (Edinburgh Instruments, U.K.), and visible-PMT as the detector. Emission photographs were captured under 365 nm UV lamp by a Nikon camera. Low temperature dependence PL studies were performed using assembly with FLS-1000 fluorescence spectrometer and liquid helium as coolant. Room temperature and low-temperature electron paramagnetic resonance (EPR) studies at room temperature were performed on a Bruker EMX Series spectrometer using X band frequency (9.5 GHz) and 100 kHz field modulation. Positron annihilation lifetime spectra were measured under ambient conditions on powder samples where Na-22 encapsulated between two 8 micron polyimde films was immersed in the powder. The lifetime spectrometer is constructed from two BaF_2 detectors whose signals were digitized using DDRS4PALS software.[1] The time resolution of the spectrometer was 220 ps. The positron lifetime spectra were analysed using PALSfit3 software.[2] X-Ray photoelectron (XPS) spectroscopy was performed on a KAlpha plus XPS system by ThermoFisher Scientific instruments in an ultrahigh vacuum chamber (7X10-9 torr) using Al Kα radiation (1486.6 eV).

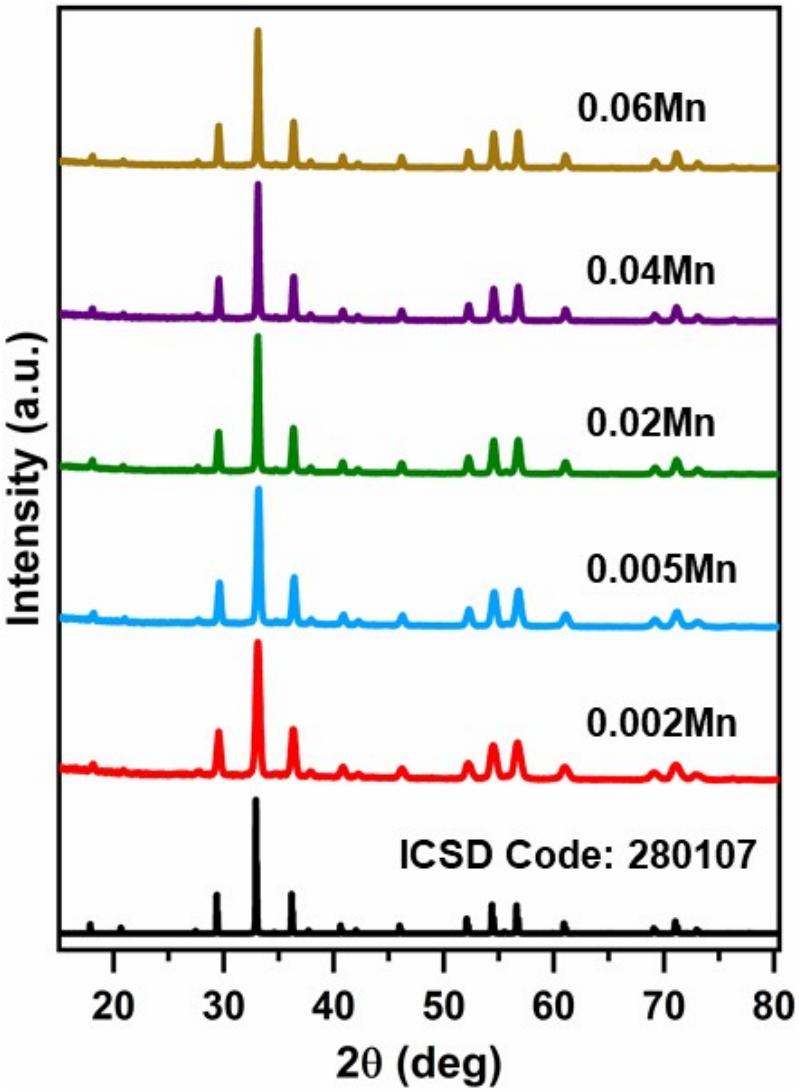

Figure S1: XRD patterns of YAGG: xMn$^{2+/4+}$ (x = 0.002, 0.005, 0.02, 0.04 and 0.06 mol) samples.

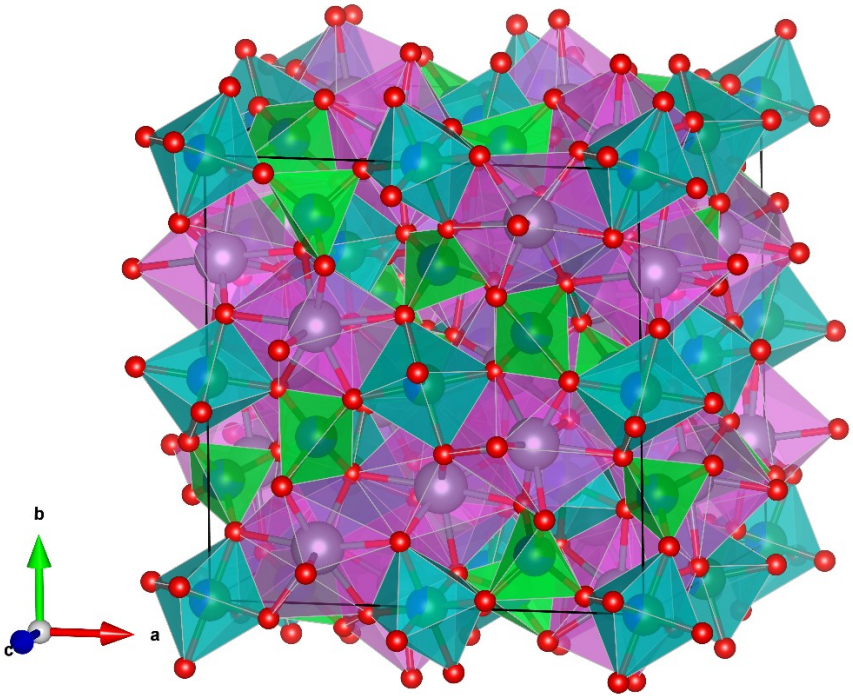

Figure S2: Crystal structure of YAGG.

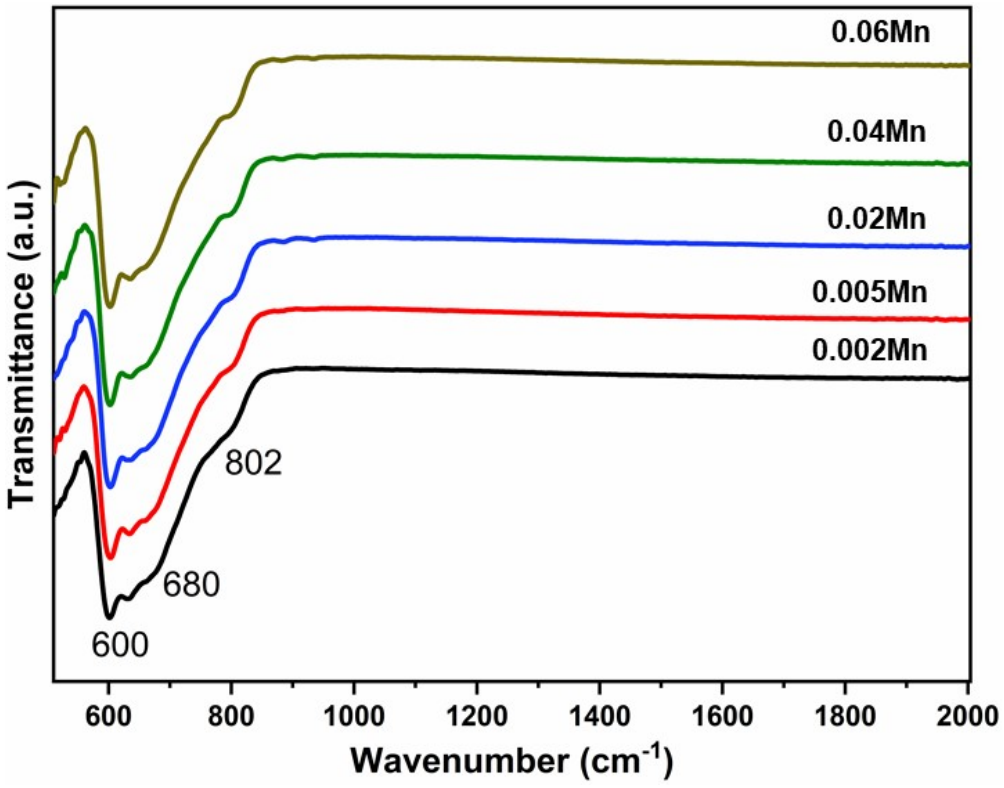

Figure S3: FTIR spectra of YAGG: xMn$^{2+/4+}$ (x = 0.002, 0.005, 0.02, 0.04 and 0.06 mol) samples.

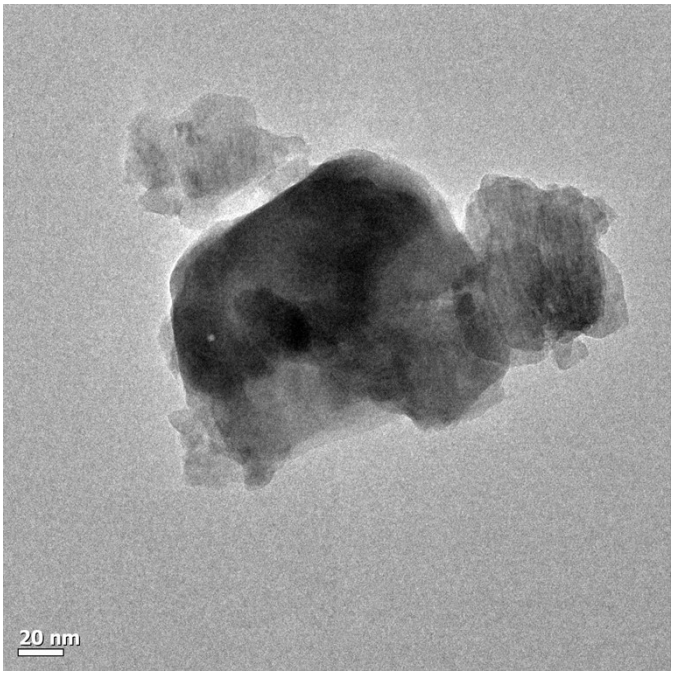

Figure S4: TEM image of YAGG:0.02Mn$^{2+/4+}$ phosphor, respectively. Scale bar: 20 nm.

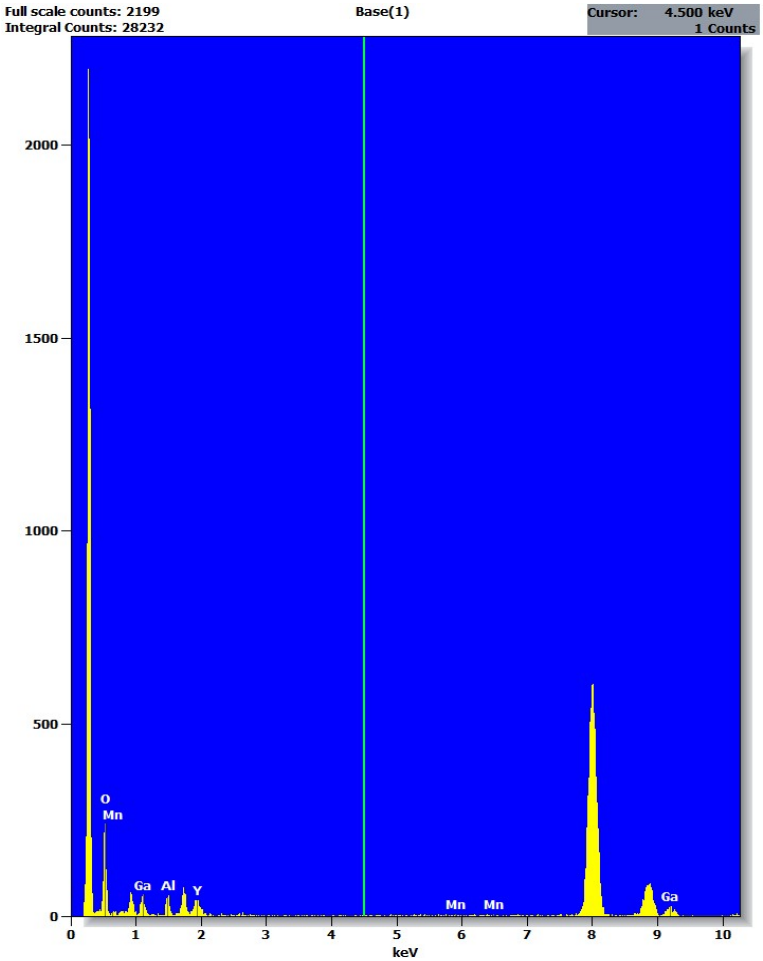

Figure S5: EDS spectra of YAGG: 0.02Mn$^{2+/4+}$ sample.

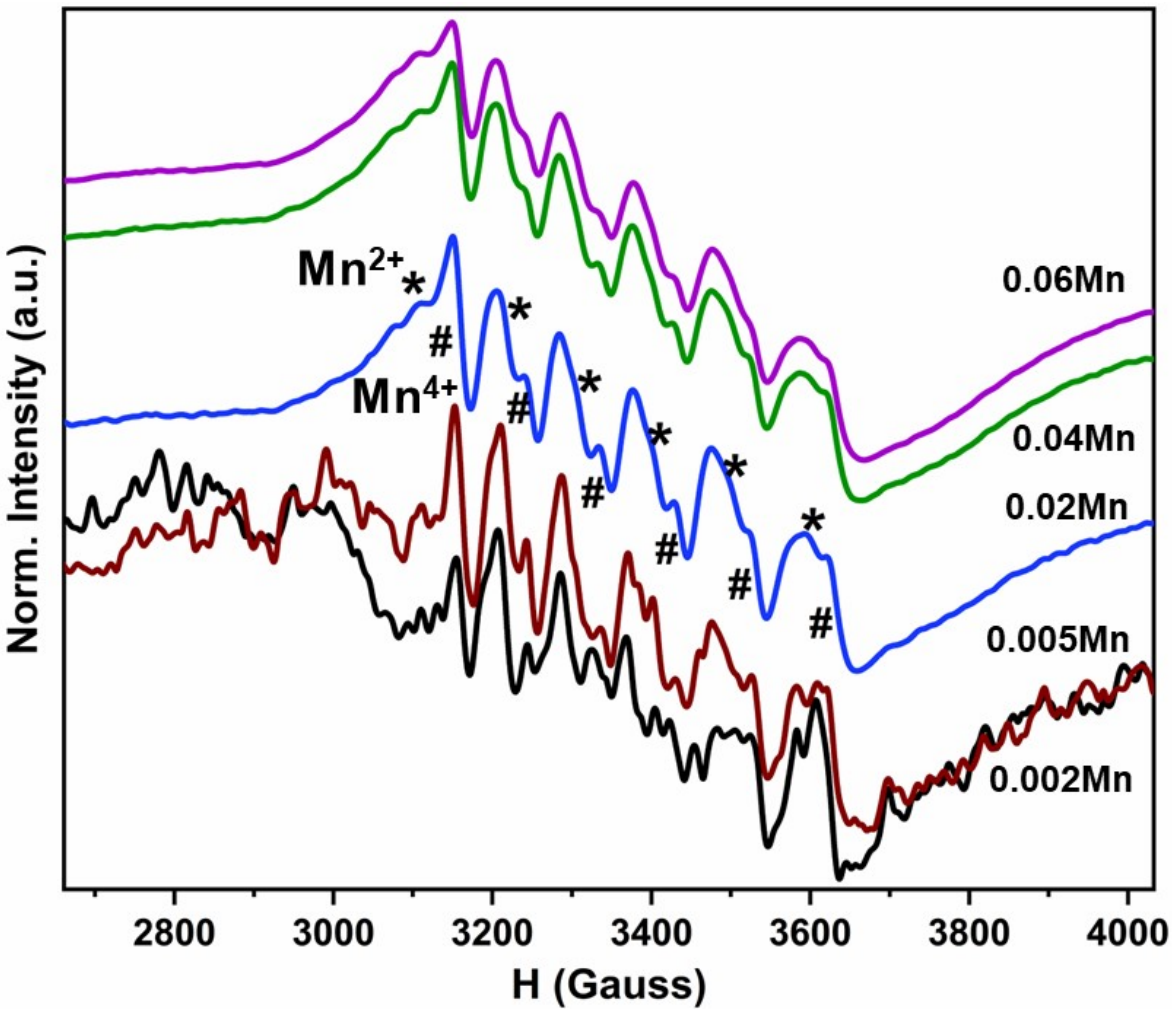

Figure S6: EPR spectra of YAGG: xMn$^{2+/4+}$ (x = 0.002, 0.005, 0.02, 0.04 and 0.06 mol) samples.

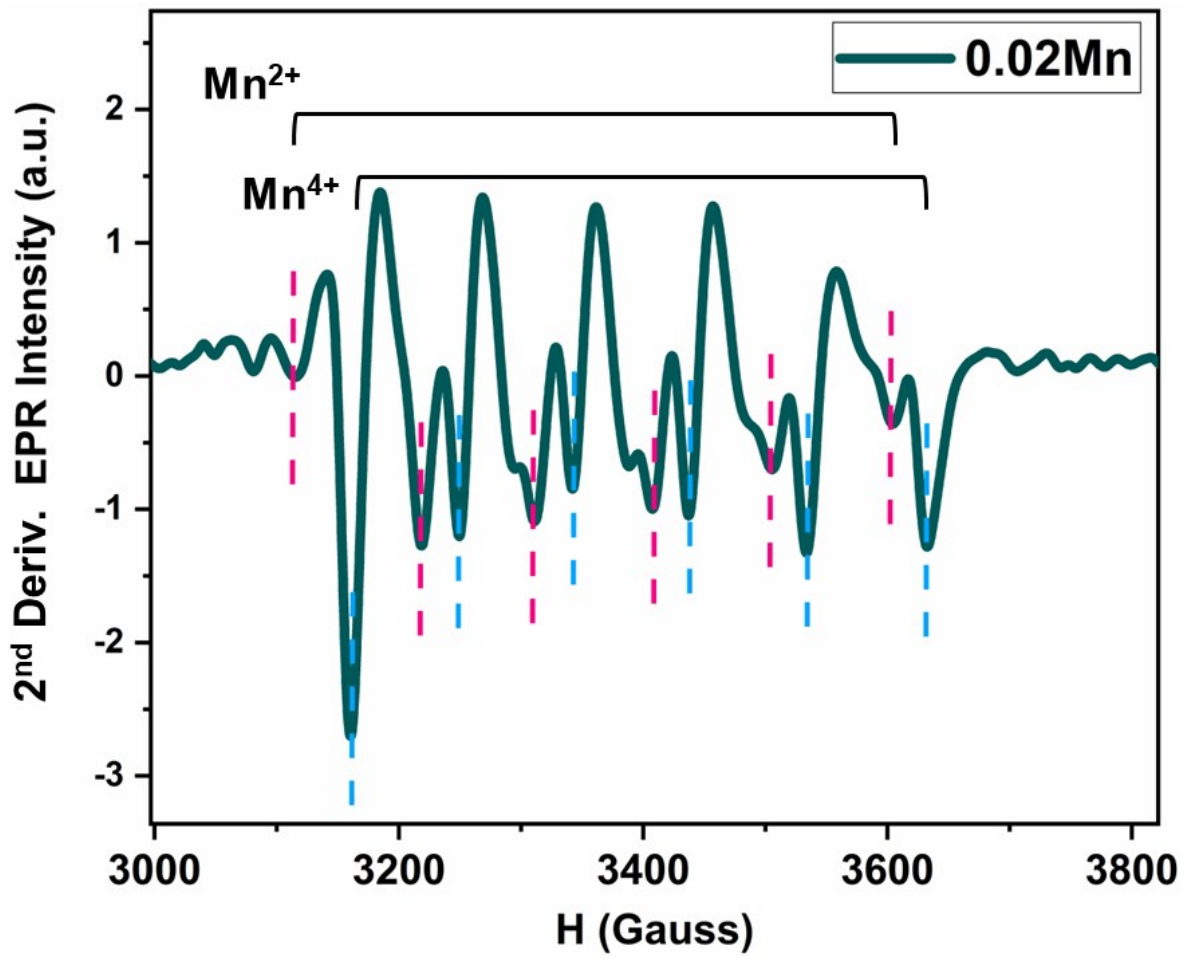

Figure S7: Double derivative of EPR intensity of YAGG: 0.02$Mn^{2+/4+}$ sample.

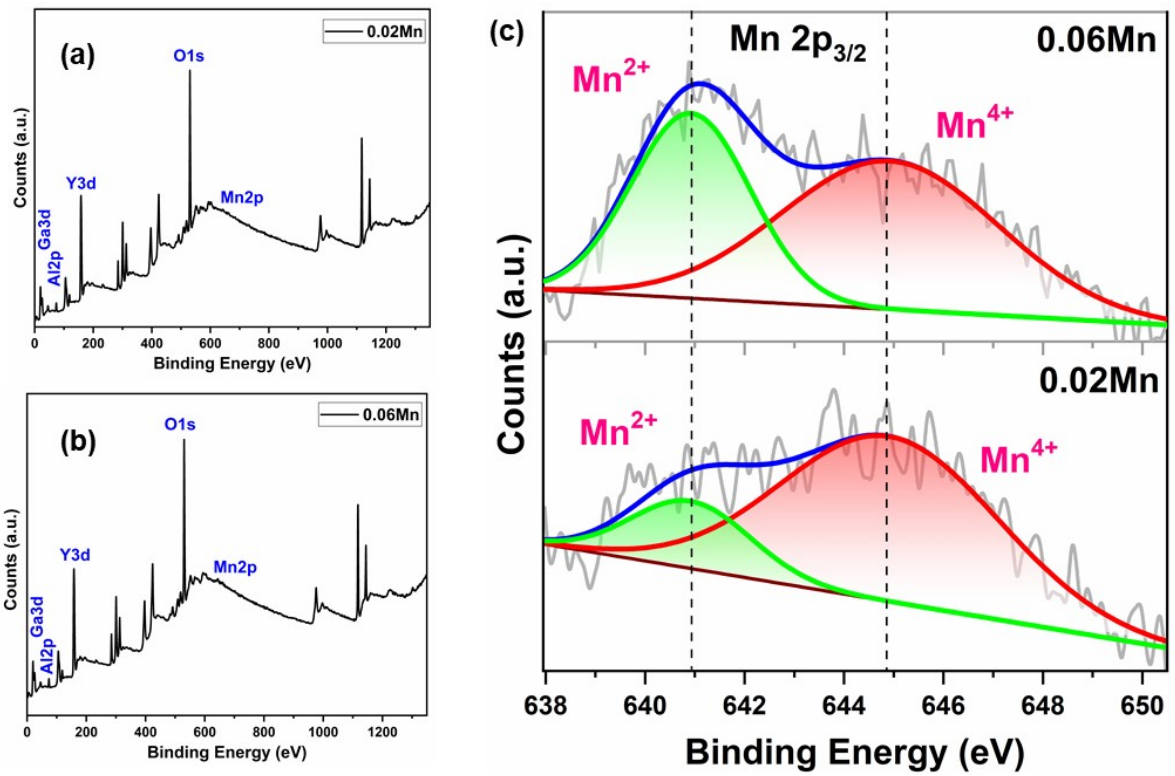

Fig. S8: (a, b) XPS survey scan of YAGG:0.02 and YAGG:0.06Mn samples and (c) XPS spectra of Mn $2p_{3/2}$.

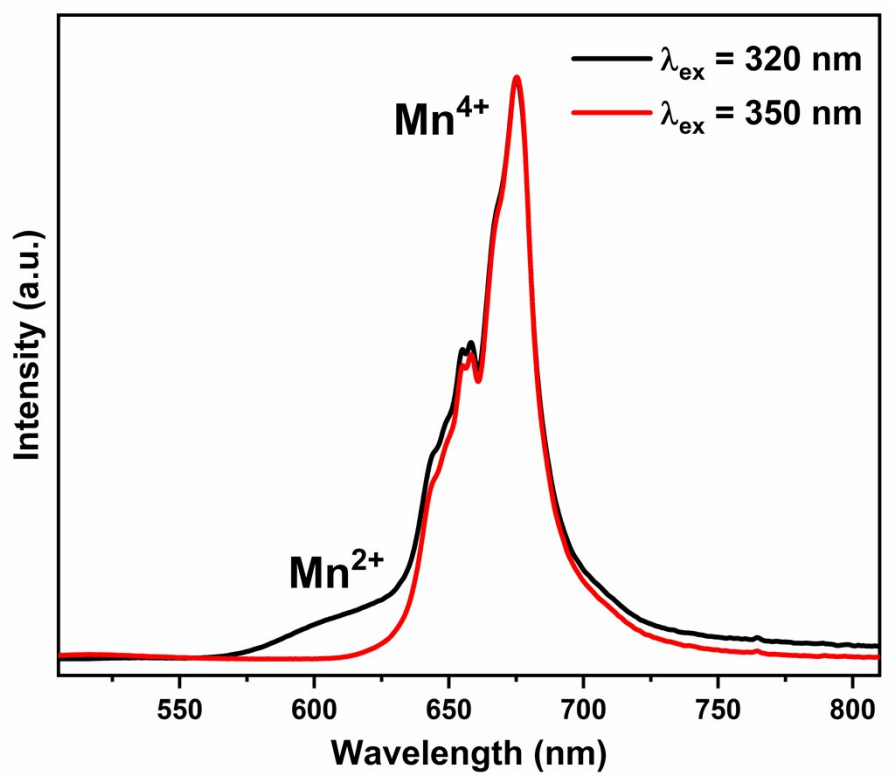

Figure S9: Normalized PL emission spectra of YAGG:0.002Mn sample under 320 and 350 nm excitations.

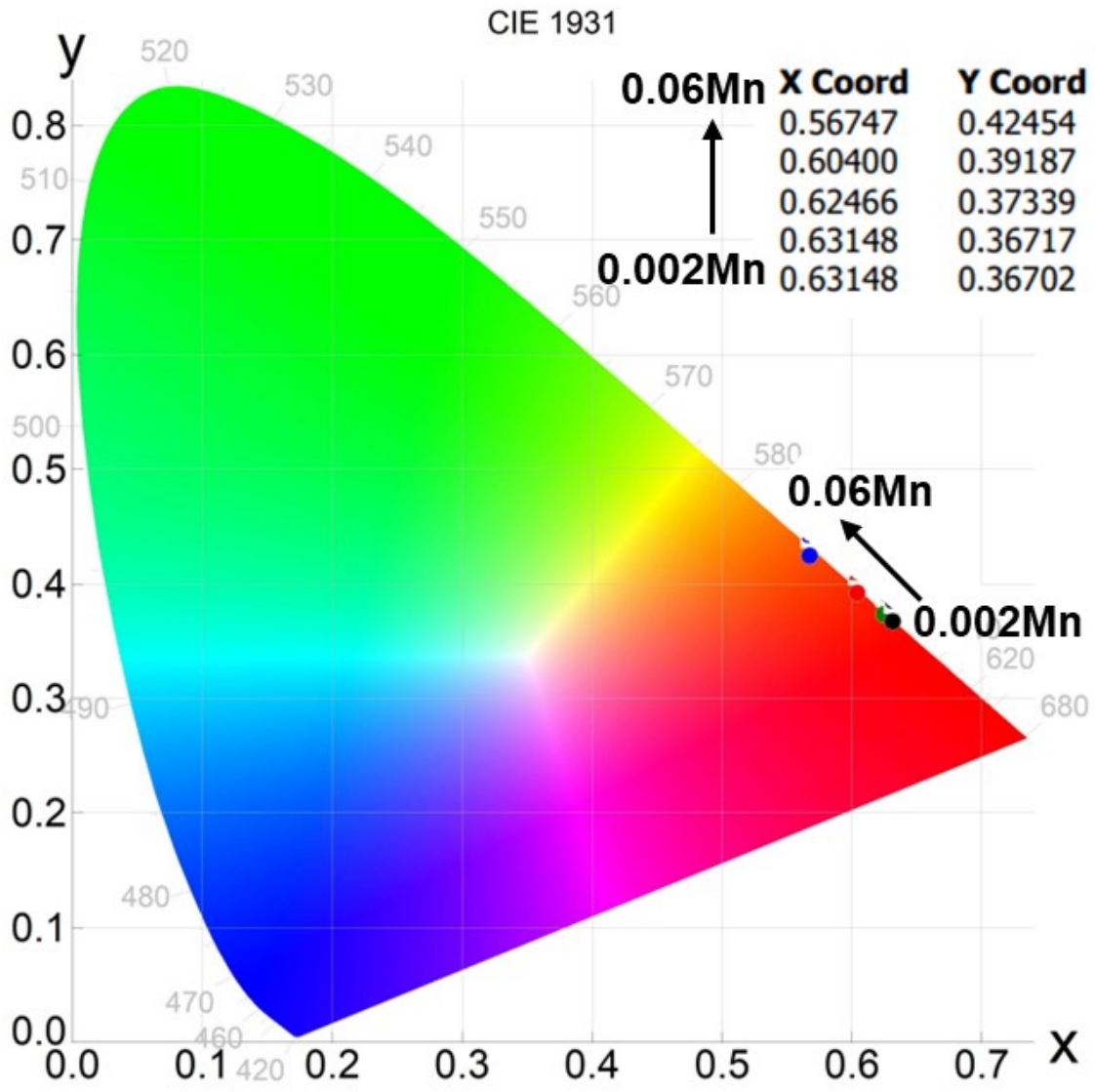

Figure S10: CIE color coordinate diagram for YAGG: xMn$^{2+/4+}$ (x = 0.002, 0.005, 0.02, 0.04 and 0.06 mol) samples (λ_{ex} = 280 nm).

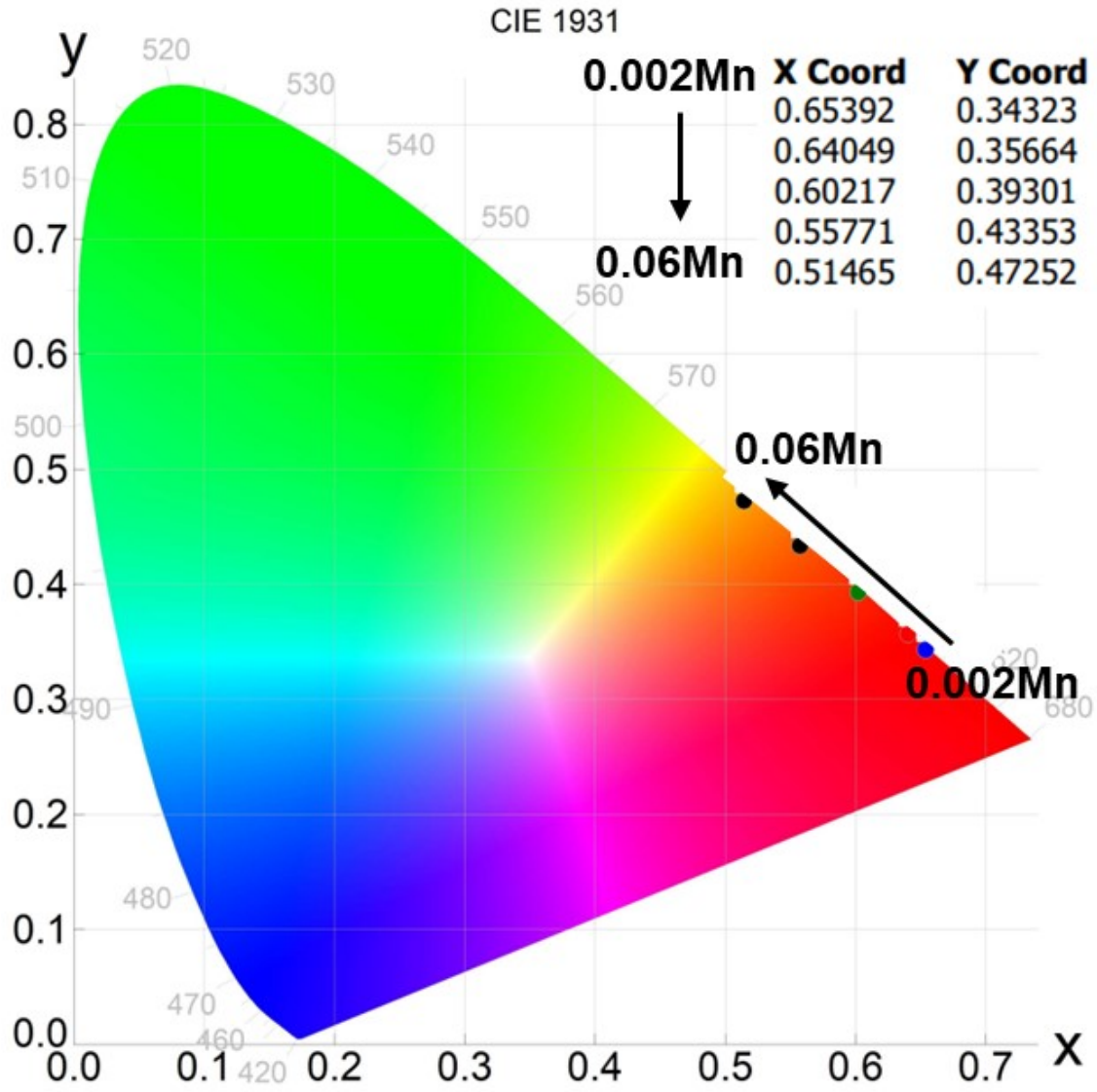

Figure S11: CIE color coordinate diagram for YAGG: xMn$^{2+/4+}$ (x = 0.002, 0.005, 0.02, 0.04 and 0.06 mol) samples (λ_{ex} = 320 nm).

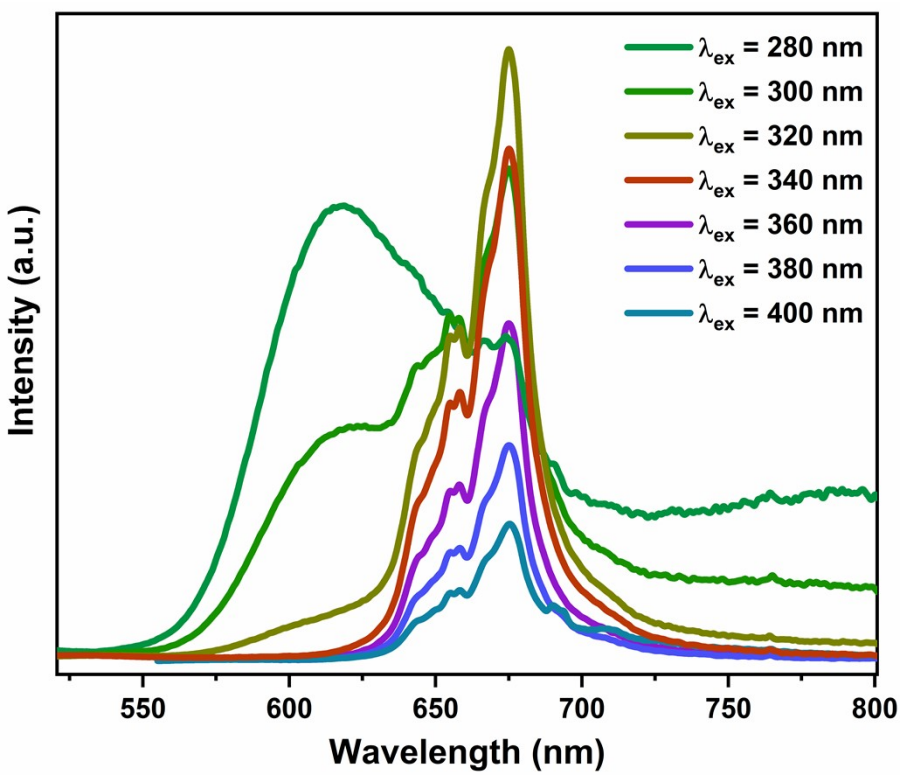

Figure S12: Excitation-dependent emission spectra for YAGG: 0.002$Mn^{2+/4+}$ sample (λ_{ex} = 280-400 nm).

S2. Concentration quenching

The mechanism of concentration quenching can be explained by different types of multipolar interactions which can be determined by using the following equation:

$$\frac{I}{x} = K[1 + \beta(x)^{\theta/3}]^{-1} \quad \text{(S1)}$$

where I and x denote the emission intensity and concentration (mol) of the Mn^{4+}/Mn^{2+} activators above the optimal concentration, K and β are constants, and θ stands for type of multipolar interaction with value of θ = 6, 8, and 10 ascribed to the dipole–dipole, dipole–quadrupole, and quadrupole–quadrupole interactions, respectively. The linear fit of log(I/x) versus log(x) is shown in **Fig. S13a** (280 nm) and **Fig. 13b** (320 nm) with θ close to 6.

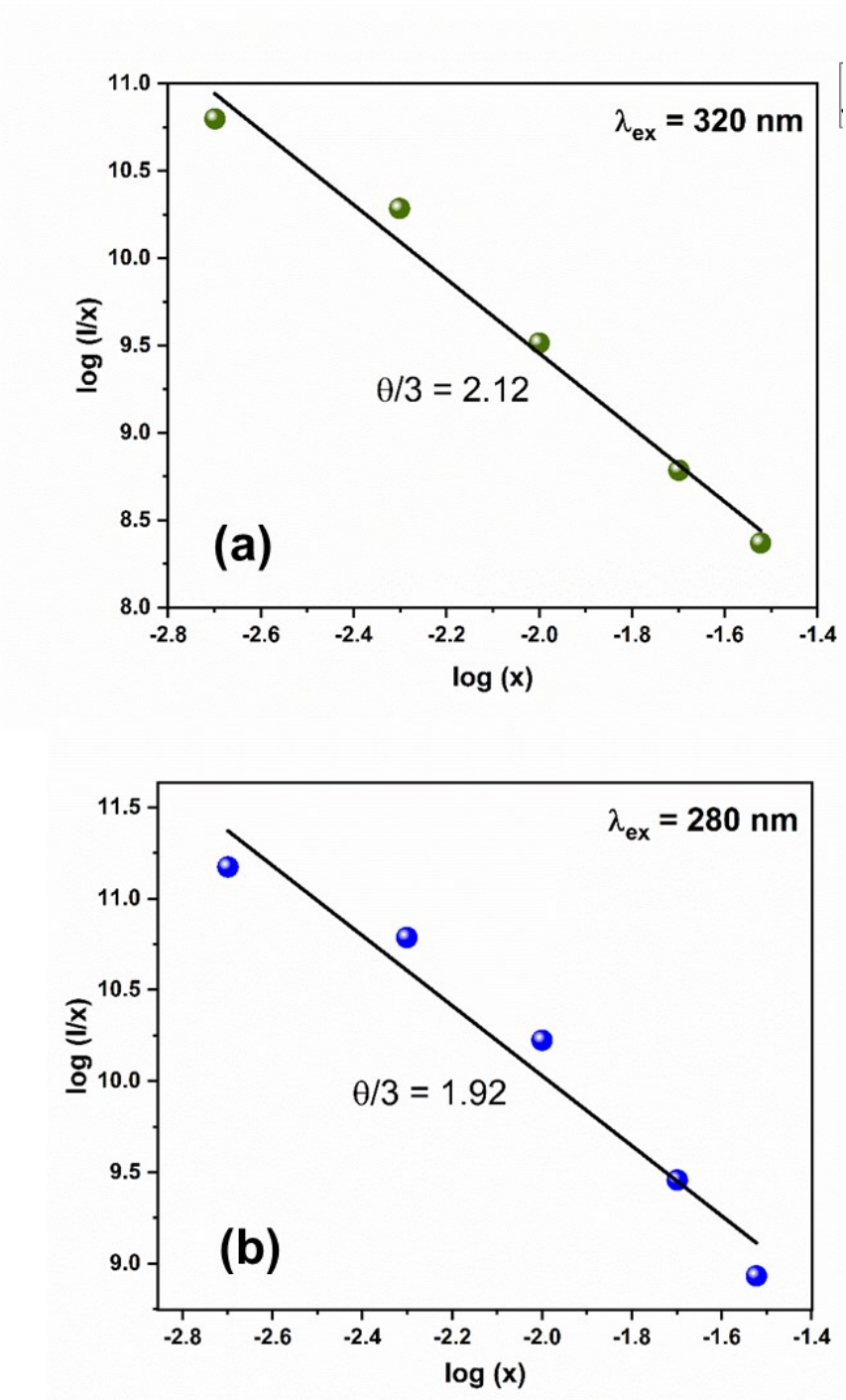

Figure S13: Dependence of log(I/x) versus log(x) for (a) λ_{ex} = 320 nm and (b) λ_{ex} = 280 nm.

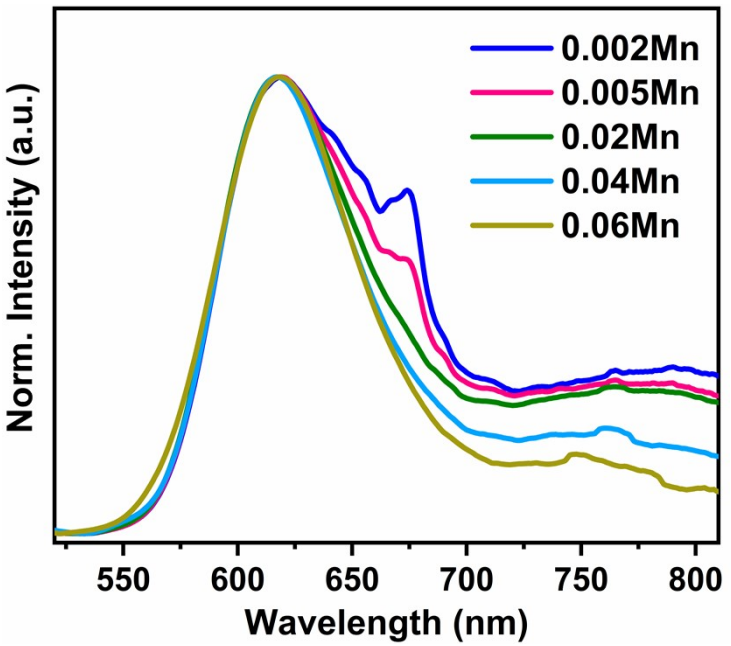

Figure S14: Normalised PL emission spectra of YAGG: xMn$^{2+/4+}$ (x = 0.002, 0.005, 0.02, 0.04 and 0.06 mol) samples (λ_{ex} = 280 nm).

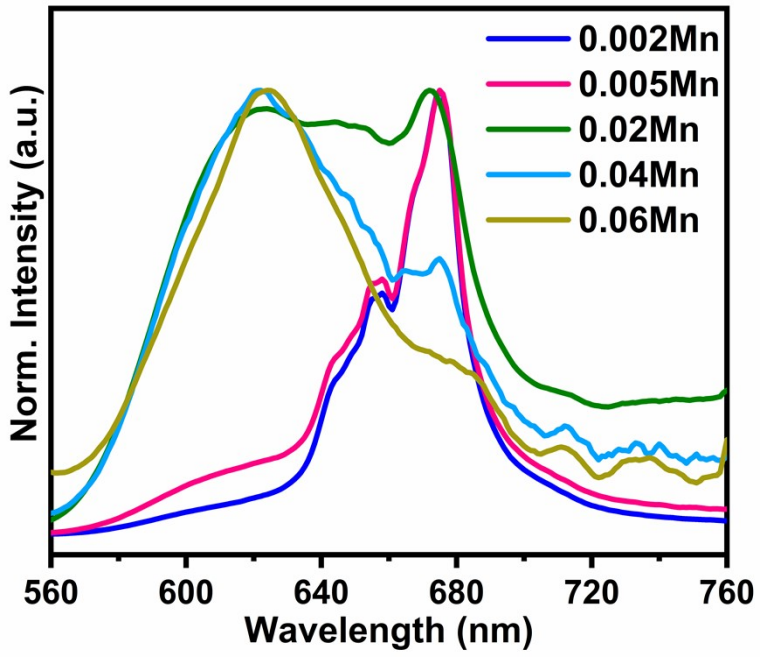

Figure S15: Normalised PL emission spectra of YAGG: xMn$^{2+/4+}$ (x = 0.002, 0.005, 0.02, 0.04 and 0.06 mol) samples (λ_{ex} = 320 nm).

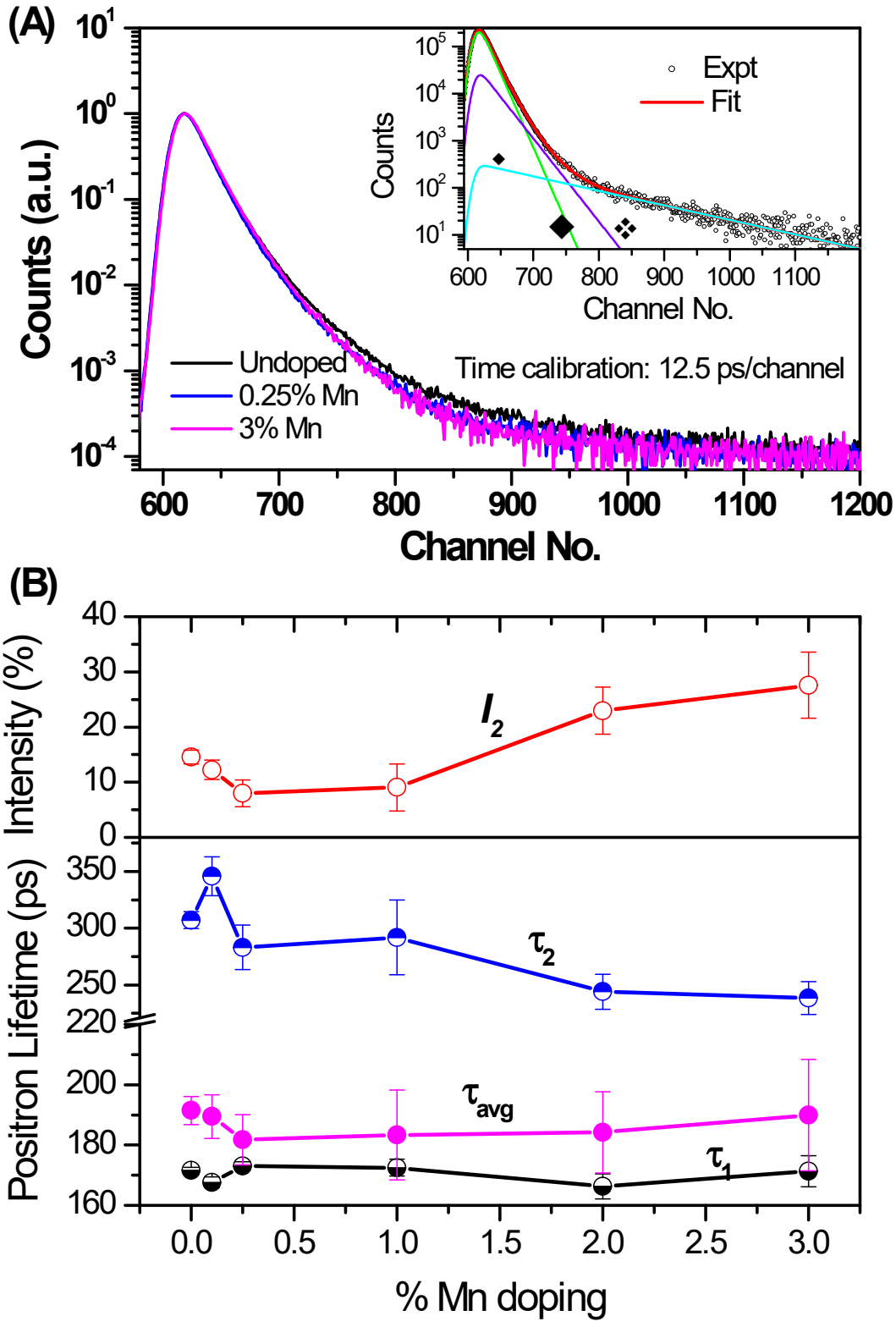

Figure S16: (a) Positron annihilation lifetime spectra from few Mn doped YAG samples. Inset shows the typical fitting of the positron annihilation lifetime spectrum to extract lifetimes, (b) Individual positron lifetimes and the intensity weighted average positron lifetimes in Mn doped YAG samples. Fractional intensity of positrons annihilating from defect states corresponding to τ_2 is also given in the top layer.

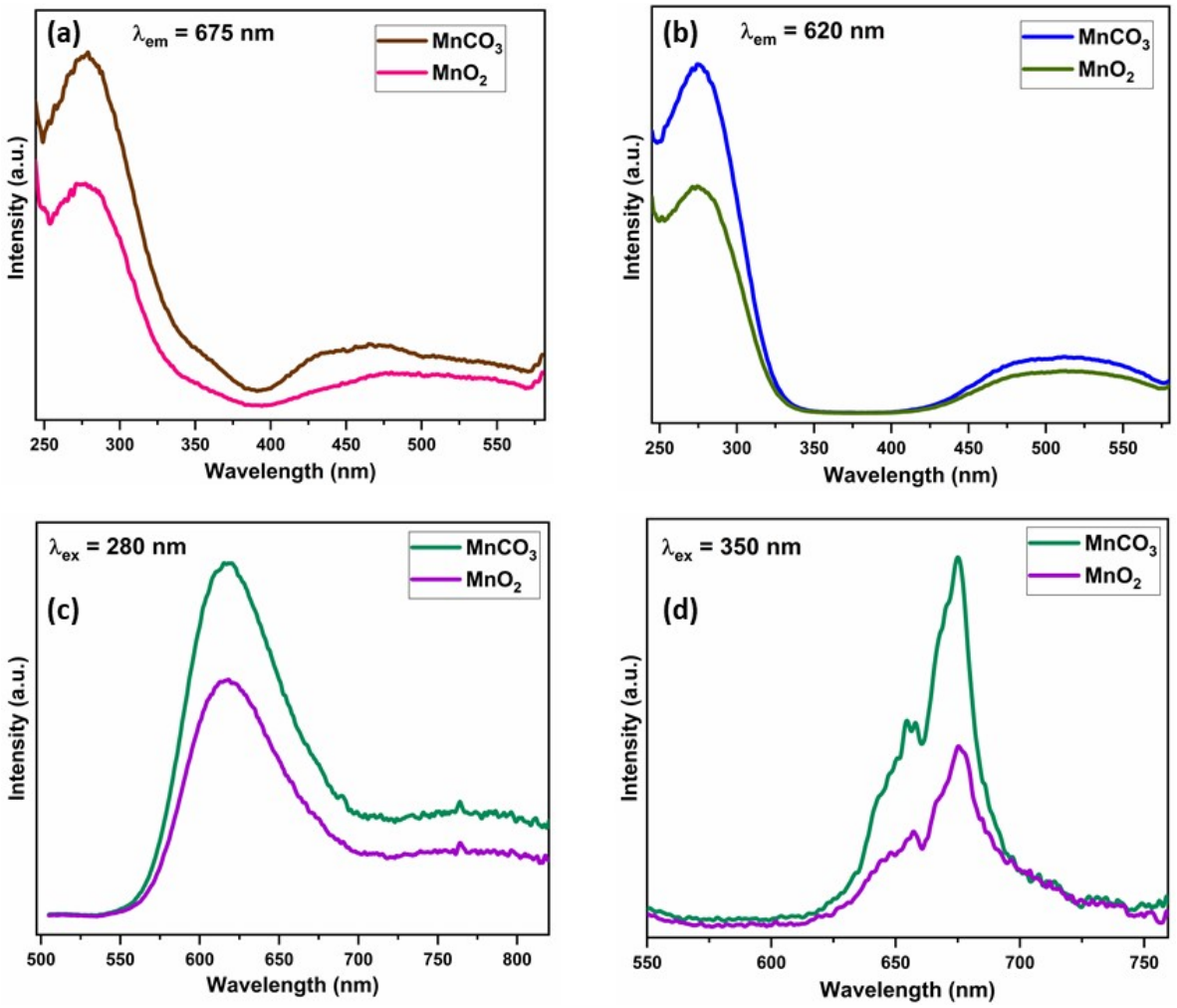

Figure S17: PLE excitation spectra of YAGG:0.02Mn samples synthesized using $MnCO_3$ and MnO_2 as raw Mn source.

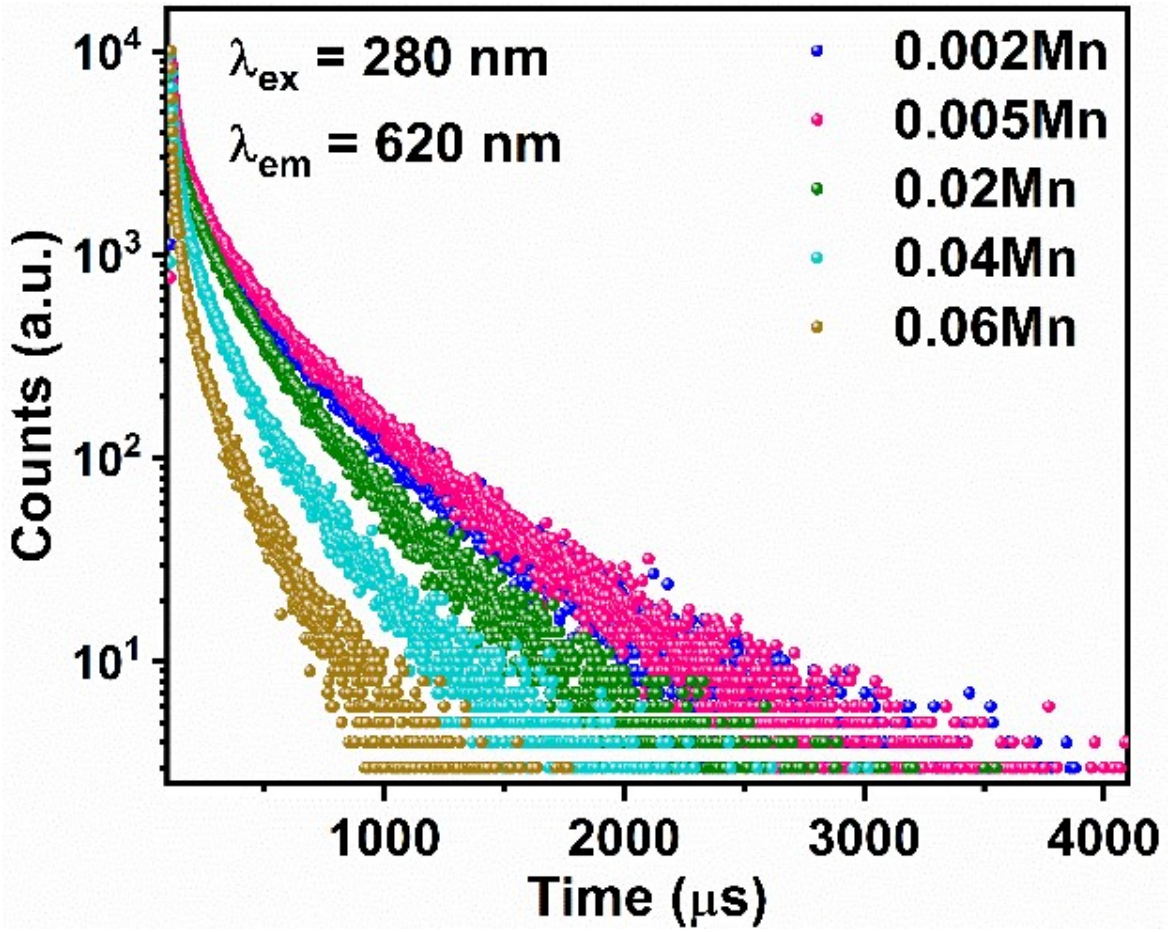

Figure S18: Decay curves of Mn ions at λ_{ex} = 280 nm and λ_{em} = 620 nm.

Table S1: Lifetime values of Mn ions at different excitation and emission wavelengths.

λ_{ex} = 280 nm and λ_{em} = 620 nm					
Sample	**τ_1 (μs)**	**%**	**τ_2 (μs)**	**%**	**τ_{avg} (μs)**
0.002 Mn	140.37	36.6	477.65	63.4	354.2
0.005 Mn	148.66	32.7	463.35	67.3	360.5
0.02 Mn	148.41	36.4	425.007	63.6	324.4
0.04 Mn	88.58	37.8	285.78	62.2	211.2
0.06 Mn	66.02	33.0	207.13	67.0	160.6
λ_{ex} = 280 nm and λ_{em} = 675 nm					
Sample	**τ_1 (μs)**	**%**	**τ_2 (μs)**	**%**	**τ_{avg} (μs)**
0.002 Mn	192.66	36.6	693.79	63.4	510.4
0.005 Mn	180.83	37.9	594.14	62.1	437.6
0.02 Mn	154.53	37.9	454.21	62.1	340.6
0.04 Mn	109.16	32.2	447.21	67.8	338.4
0.06 Mn	82.6	21.2	327.9	78.8	275.9
λ_{ex} = 320 nm and λ_{em} = 675nm					
Sample	**τ_1 (μs)**	**%**	**τ_2 (μs)**	**%**	**τ_{avg} (μs)**
0.002 Mn	233.17	30.3	833.79	69.7	651.8
0.005 Mn	244.23	29.9	827.88	70.1	653.4
0.02 Mn	168.26	37.4	566.63	62.6	417.8
0.04 Mn	109.16	32.2	447.21	67.8	338.3
0.06 Mn	82.6	21.2	327.9	78.8	275.9

Table S2: Lifetime values of Mn ions at 350 nm excitation and 675 nm emission wavelengths.

λ_{ex} = 350 nm and λ_{em} = 675nm					
Sample	τ_1 (μs)	%	τ_2 (μs)	%	τ_{avg} (μs)
0.002 Mn	185.7	28.6	729.7	71.4	574.1
0.005 Mn	185.9	29.8	732.2	70.2	569.4
0.02 Mn	111.1	29.0	452.7	71.0	353.6
0.04 Mn	77.7	29.9	445.9	70.1	335.8
0.06 Mn	35.3	18.7	239.0	81.3	200.9

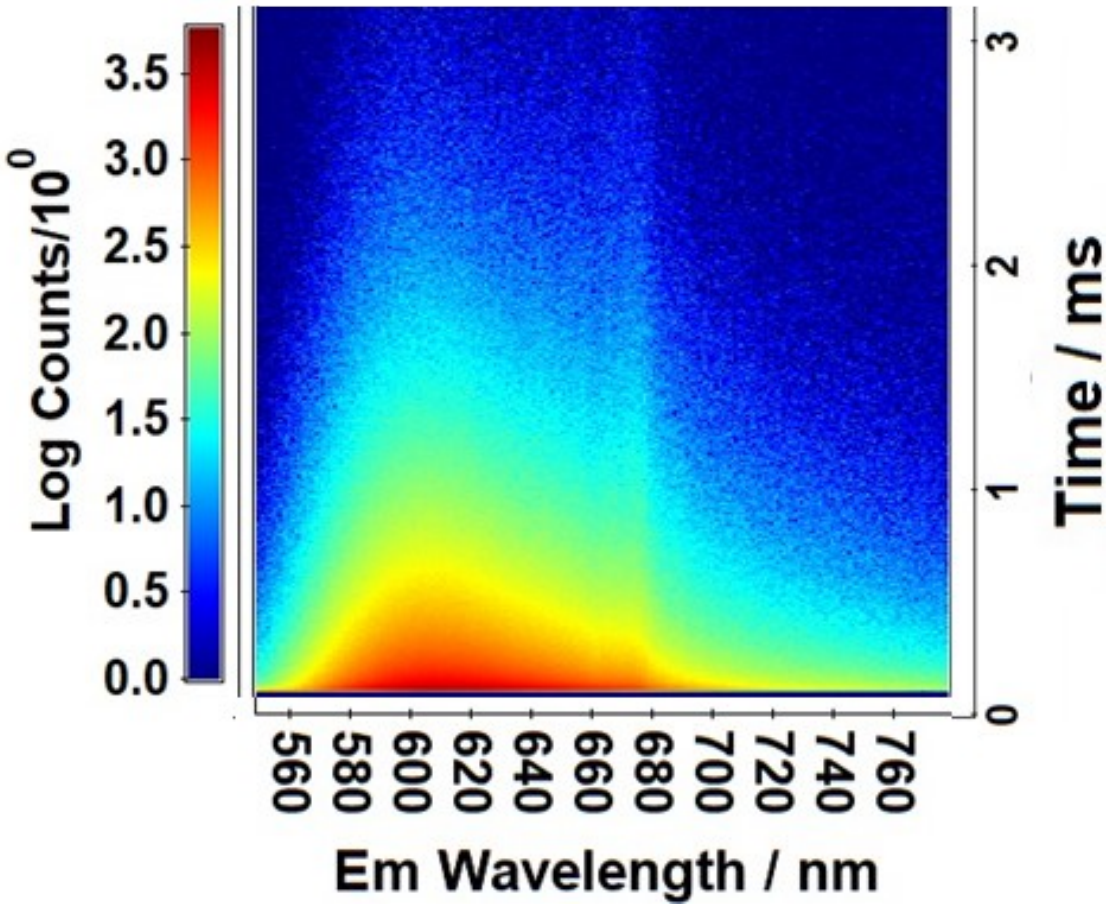

Figure S19: TRES spectra of YAGG:0.002Mn (λ_{ex} = 280 nm).

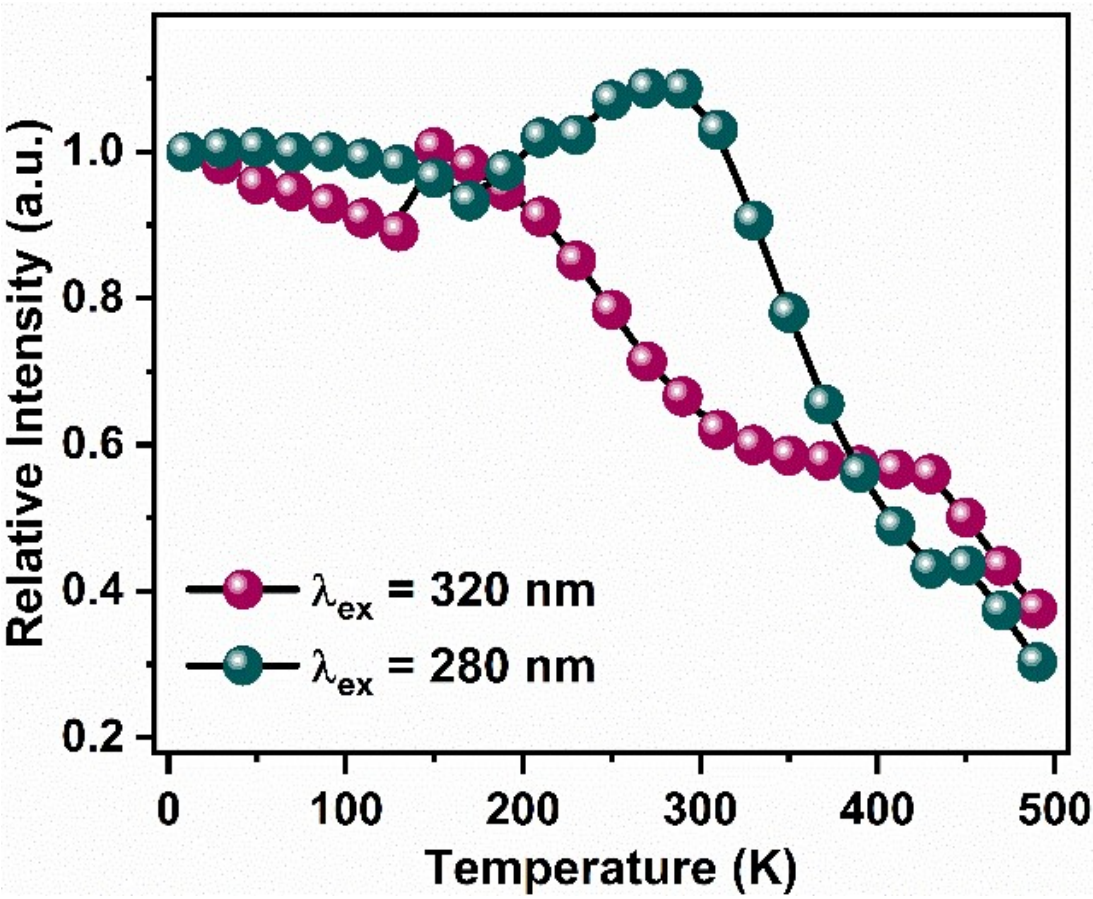

Figure S20: Change in the total integral emission intensity at λ_{ex} = 320 nm and λ_{ex} = 280 nm as a function of temperature.

S3. Activation energy for thermal quenching

The equation described by Shibata *et al*[3]. model is

$$I_T = I_0\left(\frac{1 + Aexp(-\Delta E_1/kT)}{1 + Cexp(-\Delta E_2/kT)}\right) \quad \text{(S2)}$$

where I_0 and I_T are initial intensity and intensity at temperature, T, k is Boltzmann constant, ΔE_1 and ΔE_2 are the activation energy for anti-thermal quenching (TQ) and TQ processes, A and C are constants, respectively.

The TQ of 675 nm emission can fitted using the Arrhenius equation:

$$I_T = I_0/(1 + Aexp(-\Delta E_3/kT)) \quad \text{(S3)}$$

where ΔE_3 is the activation energy for thermal quenching and A is a constant.

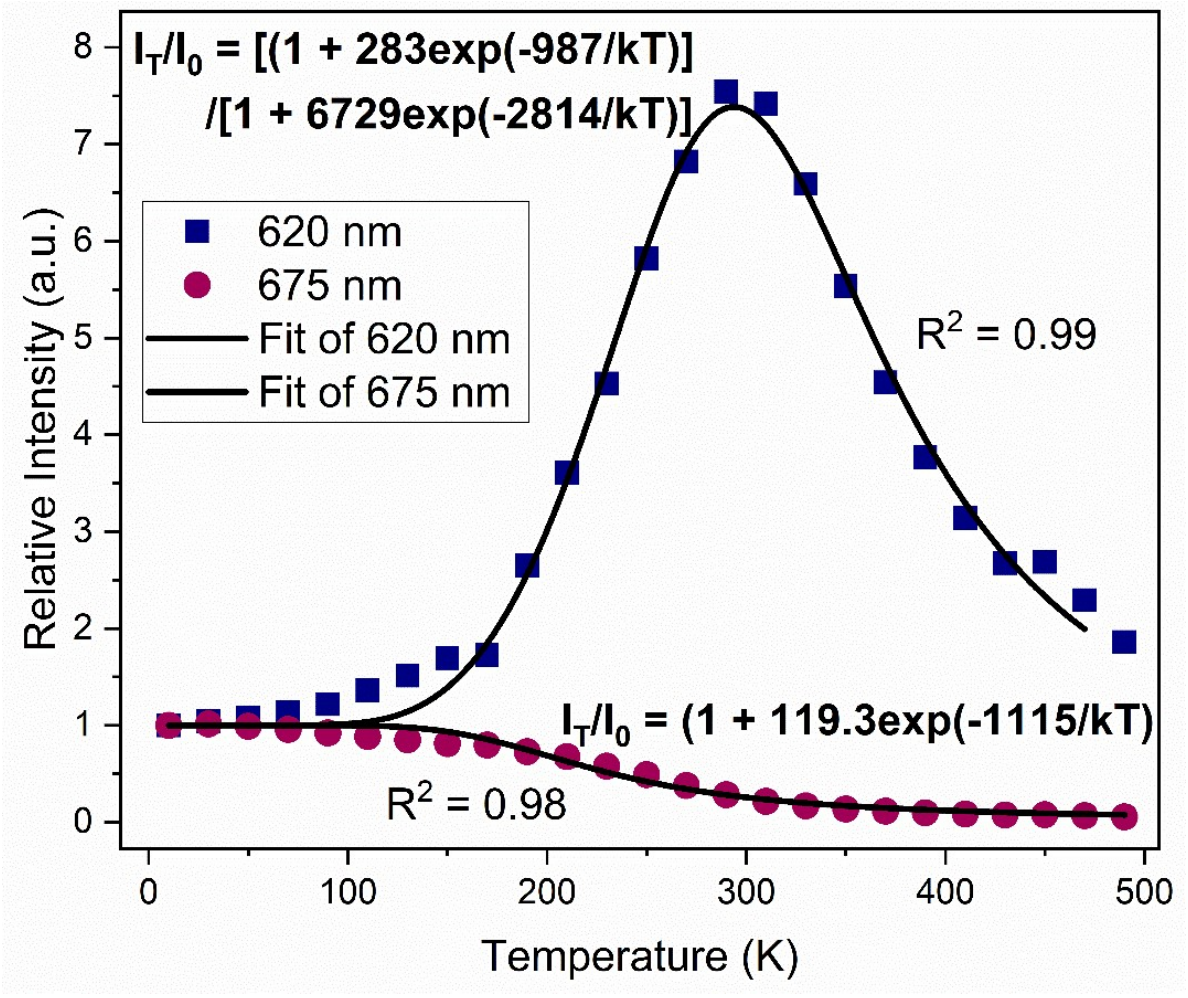

Figure S21: Fitting curves of temperature-dependent emission intensities at 620 and 675 nm under 280 nm excitation.

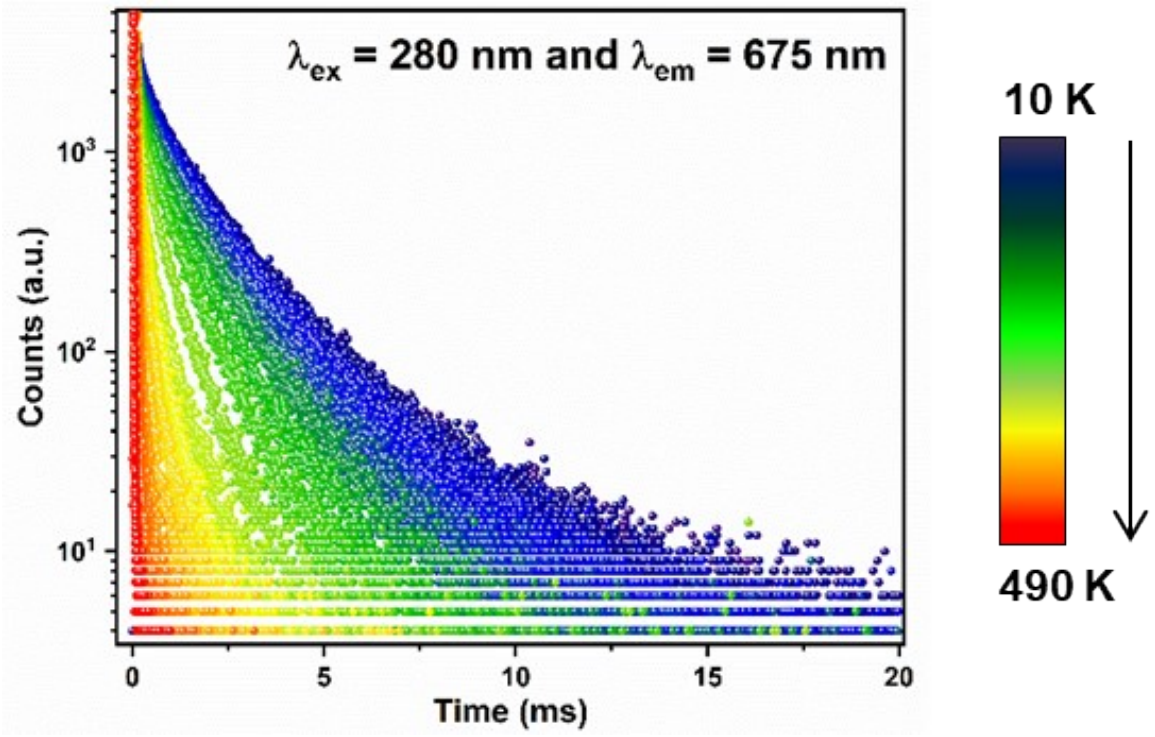

Figure S22: Luminescence decay profiles as a function of temperature at λ_{ex} = 280 nm and λ_{em} = 675 nm.

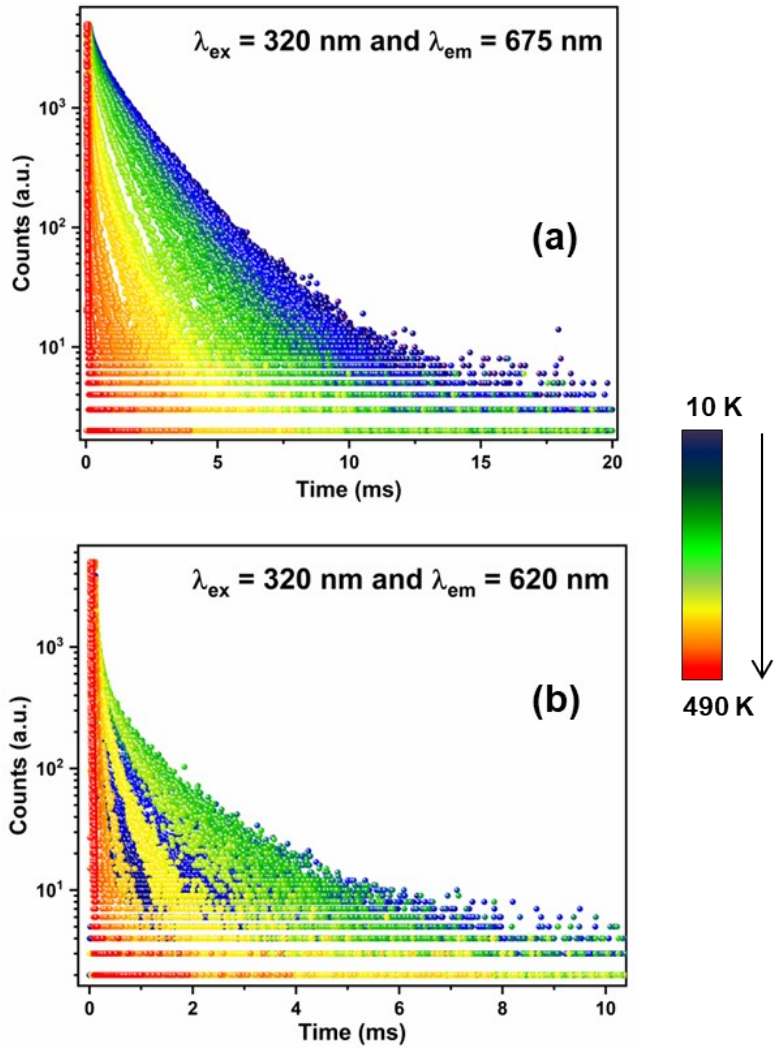

Figure S23: Luminescence decay profiles as a function of temperature at λ_{ex} = 320 nm for (a) λ_{em} = 675 nm and (b) λ_{em} = 620 nm.

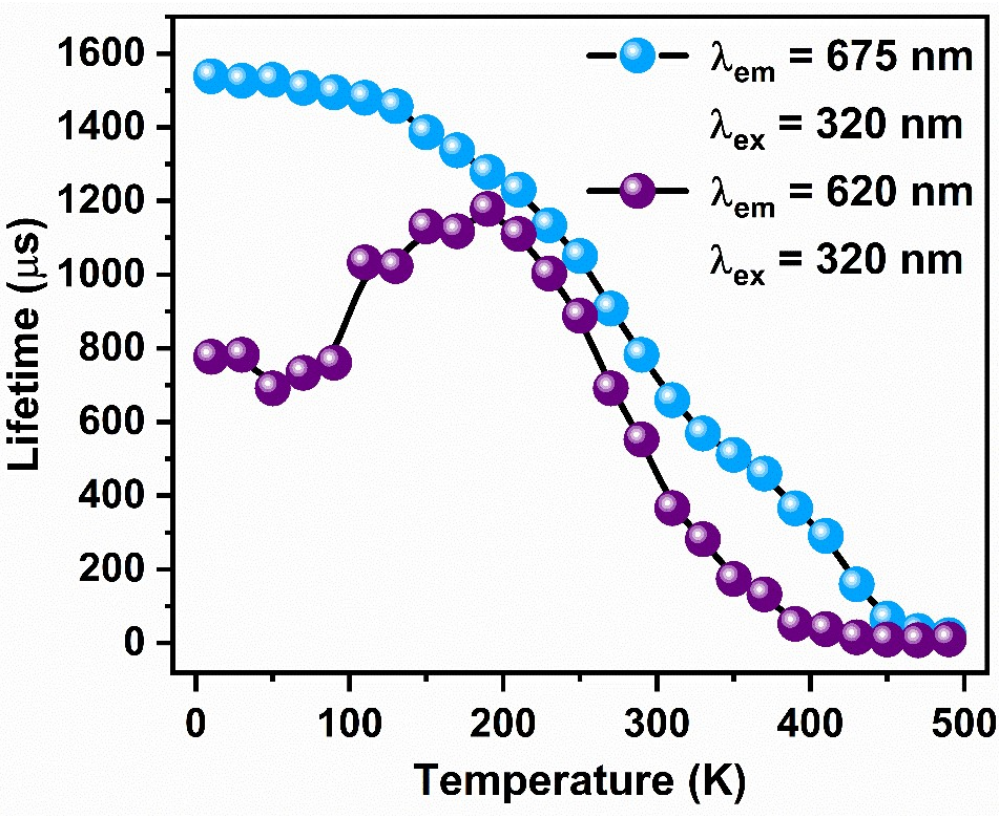

Figure S24: Temperature variation of lifetime for λ_{ex} = 320 nm.

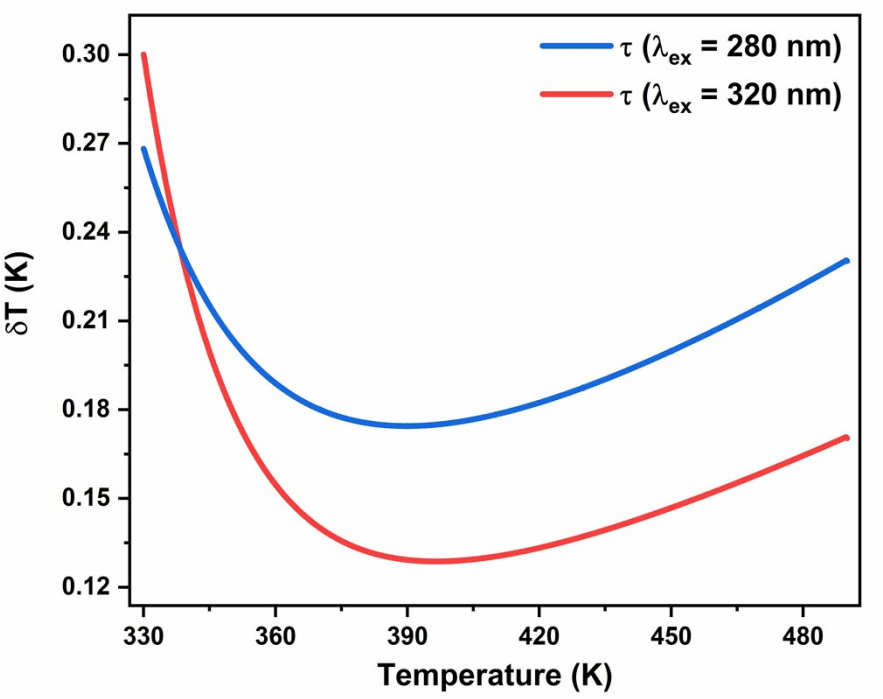

Figure S25: Temperature resolution, δT in the temperature range from 330 to 490 K for lifetime thermometry.

References:

1. D. Petschke and T. E. Staab, *SoftwareX*, 2019, **10**, 100261.
2. J. Olsen, P. Kirkegaard and M. Eldrup, 2019.
3. H. Shibata, *Japanese Journal of Applied Physics*, 1998, **37**, 550.